

Utilizing Decision Tree-Based Patterns For Predicting Building Energy Consumption

Juxian Xiao* and Zhentao Zhang

Department of Architectural Engineering, Shijiazhuang College of Applied Technology, Shijiazhuang, 050081, China

* Corresponding author. E-mail: xiaojx1999@163.com

Received: December 04, 2023; Accepted: August 04, 2024

Efficiently managing building heating loads (HL) is essential for maximizing energy use and reducing environmental impact. This study explores the application of decision tree (DT)-based patterns in predicting HL, coupled with two innovative optimizers, the Cheetah Optimization Algorithm (COA) and Smell Agent Optimization (SAO). The research leverages the flexibility and interpretability of DT, a machine learning framework, to framework complex relationships between various building parameters and HL. DTs excel at capturing non-linear relationships, making them suitable for such applications. Incorporating the COA and SAO optimizers introduces an element of intelligence into the framework process. Preliminary outcomes indicate that the combination of DT with COA and SAO optimizers significantly improves the accuracy of HL prediction. This enhancement has promising implications for building management systems, allowing for more precise control of heating systems and energy consumption optimization. Significantly, the hybrid DT+SAO (DTSA) framework delivers reliable outcomes for HL prediction, boasting an impressive correlation coefficient (R^2) value of 0.996 as well as a low root mean squared error (RMSE) value of 0.657. This study advances the broader field of energy-efficient building regulation by showcasing the potential of machine learning frameworks and intelligent optimization algorithms for accurately forecasting HL.

Keywords: Heating load; Decision Tree; Cheetah Optimization Algorithm; Smell Agent Optimization

© The Author(s). This is an open-access article distributed under the terms of the [Creative Commons Attribution License \(CC BY 4.0\)](https://creativecommons.org/licenses/by/4.0/), which permits unrestricted use, distribution, and reproduction in any medium, provided the original author and source are cited.

[http://dx.doi.org/10.6180/jase.202507_28\(7\).0013](http://dx.doi.org/10.6180/jase.202507_28(7).0013)

1. Introduction

Research focused on enhancing building energy efficiency has recently been increasingly emphasized [1]. Growing concerns about energy waste and its protracted negative environmental repercussions explain why this topic is receiving more attention [2]. Buildings account for a sizable portion of greenhouse gas and energy consumption outputs; thus, experts have been working nonstop to find ways to improve building efficiency and lessen its negative effects on the environment [3]. Achieving energy savings in buildings requires the development of a range of strategies for efficient energy management [4]. Accurate energy consumption forecasting is a crucial component of these

tactics, and it's a topic that has attracted a lot of attention lately [5]. It becomes feasible to formulate specific and efficient energy conservation measures by precisely monitoring variations in building energy usage [6]. They detect and address operational inefficiencies and potential opportunities for energy conservation [7]. To reduce waste, increase energy efficiency, and ensure the proper operation of these frameworks, estimative insights are used [8]. Studies have shown that even slight improvements in the prediction of building energy consumption can lead to significant reductions in energy usage [9]. Making well-informed decisions and proactively optimizing energy usage becomes possible when energy consumption patterns are accurately estimated [10]. These steps, which are advantageous to

building managers and residents, may include improving lighting, scheduling Heating, Ventilation, and Air Conditioning (HVAC) settings, installing energy-efficient equipment, and implementing behavioral adjustments to match energy-saving goals [11].

Accurately predicting the energy consumption of buildings is a critical element of energy frameworking, yet it regularly fails to reflect actual execution [12]. Conventional energy patterns are appropriate for preliminary analysis since they estimate building energy consumption using engineering calculations according to physical laws. However, several studies have highlighted the discrepancy in energy usage between actual and projected usage, occasionally surpassing predictions by double or triple [13]. Numerical simulation frameworks are utilized for simulating building energy utilization to get around these restrictions. However, they are constrained in their ability to capture the complexities of the actual world accurately [14]. By meticulously examining the outcomes and limitations of previous research, these simulations assist in addressing the difficulties associated with the deployment of machine learning frameworks in the efficiency of building energy [15].

Patterns of artificial intelligence (AI) have the potential to significantly contribute to improving and forecasting building energy use [16]. With the use of real-time sensor inputs, historical data, and machine learning algorithms, these patterns offer precise projections and insightful recommendations for effective energy management. Over time, forecasting energy usage has advanced significantly. To effectively predict energy demand, researchers and practitioners have enhanced a variety of tools and strategies [17].

Afzal et al. used a multilayer perceptron neural network to forecast cooling and heating needs. They utilized a hybrid approach by integrating the multilayer perceptron with eight meta-heuristic algorithms for optimizing hyperparameters. Their statistical analysis identified the MLP-PSOGWO hybrid framework as the most effective, attaining high accuracy (R^2 values of 0.998 for the heating load and 0.966 for the cooling load). This study highlighted the efficacy of meta-heuristic optimizers in enhancing predictive accuracy [18]. Moradzadeh et al. employed MLP and Support Vector Regression (SVR) to forecast heating and cooling loads in residential buildings. They utilized simulated datasets where building technical parameters were input variables and heating and cooling loads were output variables. The study demonstrated that MLP excelled in predicting heating loads (R -value of 0.9993), while SVR performed better for cooling loads (R -value of 0.9878),

showcasing the strengths of these frameworks in regression tasks [19]. In a separate study, Roy et al. introduced a deep neural network (DNN) framework specifically designed to predict the need for cooling and heating in residential buildings. The DNN framework was contrasted with Minimax Probability Patterns Machine Regression (MPMR), Gradient-Boosted Machine (GBM), and Gaussian Process Regression (GPR). The research discovered that there was a high variation accounted for (VAF) in both the DNN and GPR patterns, indicating their effectiveness in capturing the variability in heating and cooling load predictions [20].

Wai et al. aimed to provide a thorough overview of the application of deep learning (DL) in water quality (WQ) management, focusing on developments from 2011 to 2022. The study emphasizes the critical importance of maintaining excellent water quality for sustainable water resource development, aligning with the United Nations' Sustainable Development Goals. It explores various DL patterns such as long short-term memory networks (LSTMs), recurrent neural networks (RNNs), and convolutional neural networks (CNNs). The research discusses optimization approaches, hybridization of DL patterns, and relevant data pre-processing frameworks essential for effective DL-based forecasting of WQ parameters in different water bodies. Notably, Wai et al.'s paper stands out as the first comprehensive study to extensively discuss the application of DL patterns specifically for forecasting WQ parameters. It highlights the transformative impact of technologies like the Internet of Things (IoT) and cloud computing on revolutionizing DL approaches in WQ management [21]. On the other hand, Liu et al. conducted research focusing on building energy consumption forecasts and their implications for energy control, design optimization, retrofit assessment, and energy pricing recommendations. Their study, which reviewed 116 research papers, centered on data-driven approaches using machine learning algorithms for predicting building energy consumption. The key findings of Liu et al.'s research underscore the significant role of outdoor dry-bulb temperature in influencing building energy usage patterns. They cover prediction frameworks applicable across different building levels, time scales, and types of energy usage. The study emphasizes the importance of hyperparameter optimization, data pre-processing frameworks tailored for time-scale prediction, and effective feature extraction from energy consumption data to enhance prediction accuracy [22].

In this investigation, a new machine-learning approach is introduced that is designed to attain precise and optimal prognostic outcomes. This investigation's hybridization strategy is specifically designed to improve DT patterns'

execution and provide consistent outcomes. Combining two sophisticated and effective optimization frameworks, these pioneering hybrid patterns have exceeded traditional approaches, marking a significant advancement. These patterns were thoroughly evaluated to ensure an unbiased assessment of their capabilities, encompassing their standalone and hybrid configurations. Furthermore, with the deliberate decision to employ two separate optimizers, specifically the Cheetah Optimization Algorithm (COA) and Smell Agent Optimization (SAO), the goal in the construction of the hybrid patterns was to maximize each optimizer's distinct capabilities in order to improve execution.

In general, incorporating DT patterns with advanced optimization algorithms such as the COA and SAO into building HL management is both necessary and significant for several reasons. Traditional frameworks for predicting HL often fall short of capturing the complex and non-linear connection between various building parameters and HL. DT patterns, known for their ability to handle non-linearities and provide high interpretability, offer a robust solution to this challenge.

However, while DT patterns provide a solid foundation, their predictive execution can be significantly enhanced through optimization. This is where COA and SAO come into play. These intelligent optimization algorithms refine the DT framework parameters, achieving a level of predictive accuracy that traditional frameworks or simple optimizations cannot match. The integration of COA and SAO introduces an element of intelligence, optimizing the DT patterns to better capture the complex interactions between building parameters and HL.

1.1. Research Question/Hypothesis

Can the combination of decision tree-based models with COA and SAO enhance the accuracy of heating load prediction in buildings?

This study hypothesizes that integrating these optimization algorithms with a DT model will improve prediction accuracy by better capturing the complex interactions among building parameters. Specifically, we expect that the hybrid DT+SAO (DTSA) framework will achieve higher prediction accuracy, as indicated by a higher correlation coefficient (R^2) and a lower root mean squared error (RMSE), compared to traditional methods.

2. Materials and methodology

2.1. Data Gathering

A dataset is assembled to aid in the training of machine learning patterns from the body of published literature [23]. This study used 768 samples, of which 70% belonged to

training, 15% to validation, and 15% to testing phases. The HL is the target of prediction with the inputs as follows:

1. Relative Compactness: This metric quantifies the overall compactness of the building, a factor directly impacting its heat retention and loss characteristics.
2. Surface Area (m^2): The meticulous recording of the total surface area of the structure serves as a pivotal factor in comprehending the extent of its exposure to external thermal influences.
3. Wall Area (m^2): The accurate measurement of the wall area provides information about the building's ability to transport heat and its level of thermal insulation.
4. Roof Area (m^2): Because the roof area contributes to either heat gain or loss in the building's thermal equilibrium, its inclusion in the dataset is significant.
5. Overall height (m): The vertical dimension of the building bears a direct correlation with its internal volume and, subsequently, its heating load requirements.
6. Orientation: It is crucial to comprehend the structure's direction for determining its solar exposure and, in turn, how it affects heating requirements.
7. Glazing Area (%): Understanding the dynamics of heat transmission via windows requires careful recording of the fraction of glazing or fenestration area inside the building envelope.
8. Glazing Area Distribution: The way that glass is distributed throughout the building's façade shapes the patterns of heat distribution within; hence, careful recording is necessary.

Table 1 provides statistical properties for the input variables. A scatter plot is presented in Fig. 1 to better understand how these inputs influence the output. This plot illustrates the connection between the heat load values and the input variables.

2.2. Decision Tree (DT)

Based on the principles of the ML framework, a DT serves as a powerful tool for effectively addressing categorization and regression tasks. Unlike other categorization strategies that depend on a group of attributes for one-step categorization, the DT employs a multi-level or hierarchical decision-making approach with a structure comparable to a tree [24]. As an alternative to categorization approaches that rely on a consolidated collection of characteristics for instantaneous

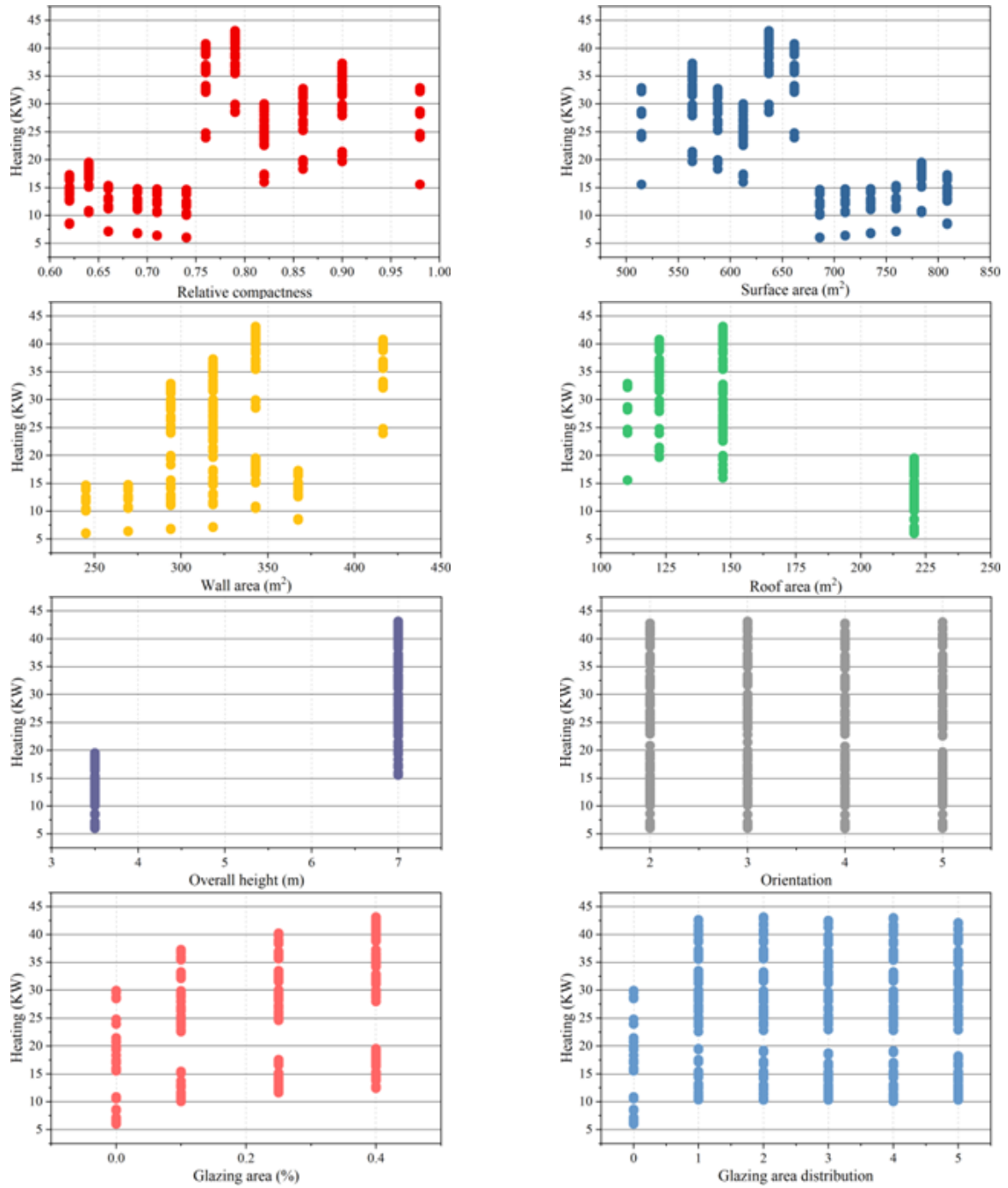
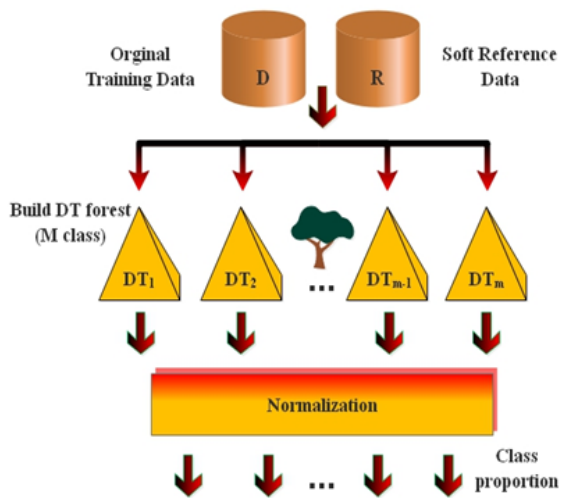


Fig. 1. Scatter plot for the relation between the input and output variables.

Table 1. Statistical properties of the input and output variables.

Variables	Category	Indicators			
		Min	Max	Avg	St. Dev.
Relative compactness	Input	0.62	0.98	0.7642	0.106
Surface area (m ²)	Input	514.5	808.5	671.71	88.09
Wall area (m ²)	Input	245	416.5	318.5	43.63
Roof area (m ²)	Input	110.25	220.5	176.60	45.17
Overall height (m)	Input	3.5	7	5.25	1.751
Orientation	Input	2	5	3.5	1.119
Glazing area (%)	Input	0	0.4	0.2344	0.133
Glazing area distribution	Input	0	5	2.8125	1.551
Heating (KW)	Output	6.01	43.1	22.307	10.09

**Fig. 2.** DT regression framework facilitates the soft categorization of remote sensing data.

categorization, the decision tree presents a tree-like structure through a multi-level or hierarchical decision-making process. This tree is made up of an array of terminal nodes (leaves), a sequence of internal nodes (splits), and the root node, which contains all the data [25]. Every node in a DT framework makes a binary choice that isolates one group or a subset of groups from the others. This usually entails using a top-down framework to navigate the tree from its highest point to its lowest point [26].

2.2.1. Decision tree regression (DTR)

To facilitate soft categorization, an individual regression tree is created for each group, as depicted in Fig. 2. In the regression trees' context, pixel intensity values across different bands are used to generate the predictor variables, also known as feature vectors. On the other hand, soft reference data is a type of data where the known group proportions of a pixel constitute the target variable or target vector. Estimated group proportions are the algorithm's output, with

intensity values for each regression tree serving as the input [27]. The procedures for developing regression trees with the training data are:

Utilize the intensity values of the pixels as predictor components derived from various bands. Use the known group percentage of group I within a pixel as the objective variable. Make a separate regression tree for group I . Repeat step 1 with integers ranging from 1 to M for group I .

For each pixel, the soft categorization outputs are converted into a range of values, ranging from 0 to 1. This range represents the group proportions inside the ground pixel region. As a result, the following process is used to normalize the expected group distributions from each tree, represented as $DT(i)$ for $i = 1, \dots, M$:

$$P(i) = \frac{DT(i)}{\sum DT(i)}, i = 1, \dots, M \quad (1)$$

2.3. Cheetah Optimization Algorithm (COA)

COA conducts a global search of nodes by borrowing tactics from how cheetahs find food. All of this may be mathematically described as a numerical framework that contains attacking, seeking, and waiting, just like a cheetah would.

$$Z_n = Z_p + k.\theta \quad (2)$$

The most recent and previous hops of the cheetah are denoted as Z_n and Z_p , respectively. In the multi-hop scenario, the cheetah's step length is symbolized as θ , and k represents the system's random parameter. During the infiltration process, the cheetah could detect the node, leading to the implementation of a sit-and-wait plan for hopping. This scenario can be

$$Z_n = Z_p \quad (3)$$

In this instance, cheetahs go to the next node in the chain by combining their quickness and agility. By limiting frequent node changes, Z_n and Z_p represent the cheetah's

previous and current nodes, respectively, preventing premature intersections. When the cheetah decides to proceed to the next node, it does so at top speed. The following describes the aggressive tactics of the cheetah:

$$Z_n = Z_B + k_1 \cdot \tau \quad (4)$$

In this instance, Z_B indicates both the present node and the optimal location for data bandwidth.

2.4. Smell Agent Optimization (SAO)

Drawing from the connection between objects emitting smell molecules and smell agents, Salawudeen et al. [28] introduced SAO as a contemporary enhancement framework.

2.4.1. Sniffing mode

Eq. (5) is employed to initiate the presence of smell molecules [29].

$$X_i^{(m)} = \begin{bmatrix} x_{(1,1)} & x_{(1,2)} & x_{(1,D)} \\ \vdots & \vdots & \vdots \\ x_{(N,1)} & x_{(N,2)} & x_{(N,D)} \end{bmatrix} \quad (5)$$

D , N , and m stand for the total count of decision variables, variables, and iterations, respectively. To get the ideal position for the agent, use Eq. (6) [30].

$$X_i^{(m)} = LB + r_0 \times (UB_i - LB_i) \quad (6)$$

A random value ranging from 0 to 1, along with the upper and lower bounds, is symbolized as r_0 , UB , and LB , respectively [31]. Eq. (7) describes the rate at which smell molecules disperse from their source.

$$v_i^{(m)} = \begin{bmatrix} v_{(1,1)} & v_{(1,2)} & v_{(1,D)} \\ \vdots & \vdots & \vdots \\ v_{(N,1)} & v_{(N,2)} & v_{(N,D)} \end{bmatrix} \quad (7)$$

The distributed molecules' velocity is modified in a Brownian manner by applying Eq. (7).

$$x_i^{m+1} = x_i^m + v_i^{m+1} \times \Delta t \quad (8)$$

Given that Δt equals 1, Eq. (9) is employed to calculate the velocity update for the smell molecules.

$$v_i^{t+1} = v_i^t + v \quad (9)$$

Eq. (10) is employed to determine the updated component of the velocity, v .

$$v = r_1 \sqrt{\frac{3kT}{M}} \quad (10)$$

T represents the temperature, k denotes the molecule mass, and M signifies the smell constant.

2.4.2. Trailing mode

To replicate the agent's movement towards smell sources, Eq. (11) is used in this mode, which describes their search behavior.

$$x_i^{m+1} = x_i^m + r_2 \times \text{olf} \times (x_{\text{agent}}^m - x_i^m) - r_3 \times \text{olf} \times (x_{\text{worst}}^m - x_i^m) \quad (11)$$

The r_2 and r_3 random variables, which range from 0 to 1, are utilized to lessen the effect of olf action property (olf) on x_{agent}^m and the impact of olf action on x_{worst}^m .

2.4.3. Random mode

The smell agent's random mobility is depicted in Eq. (12).

$$x_i^{m+1} = x_i^m + r_4 + SL \quad (12)$$

SL stands for step length and r_4 is a random value employed to mitigate its influence.

2.5. Execution Evaluators

A set of measures has been constructed in this part to assess the hybrid patterns. We may learn a lot about how well the patterns are performing from these evaluations of correlation and error. Table 2 contains the formulas for the measures utilized in this study [32].

- The symbol n is used to represent the sample size.
- Estimated values are symbolized as b_i .
- The measured value is shown as m_i .
- The means of the observed and anticipated values are denoted by \bar{m} and \bar{b} , respectively.
- The symbol \bar{x} represents the dataset's predictor variable mean.

2.6. Hyperparameters

Table 3 highlights the tailored approach taken to optimize hyperparameters for each model, DTSA and DTCO. The chosen values reflect the models' strategies to manage complexity and prevent overfitting while aiming for accurate predictions. These hyperparameters are critical for the performance of decision tree models, and the differences between DTSA and DTCO suggest that each model may be suited to different types of data or predictive tasks.

3. Outcomes and discussion

The execution of the three enhanced patterns is displayed in Table 4. In this investigation, the execution of the DT

Table 2. The Equations of the Evaluation Metrics.

Coefficient Correlation (R^2):	$R^2 = \left(\frac{\sum_{i=1}^n (b_i - \bar{b})(m_i - \bar{m})}{\sqrt{[\sum_{i=1}^n (b_i - \bar{b})^2][\sum_{i=1}^n (m_i - \bar{m})^2]}} \right)^2$
Root Mean Square Error (RMSE):	$RMSE = \sqrt{\frac{1}{n} \sum_{i=1}^n (m_i - b_i)^2}$
Mean Absolute Error (MAE):	$MAE = \frac{1}{n} \sum_{i=1}^n b_i - m_i $
Normalized Mean Square Error (NMSE):	$NMSE = \frac{1}{n} \sum_{i=1}^n \frac{(m_i - b_i)^2}{b_i \cdot m_i}$
BIAS:	$BIAS = \bar{b} - \bar{m}$

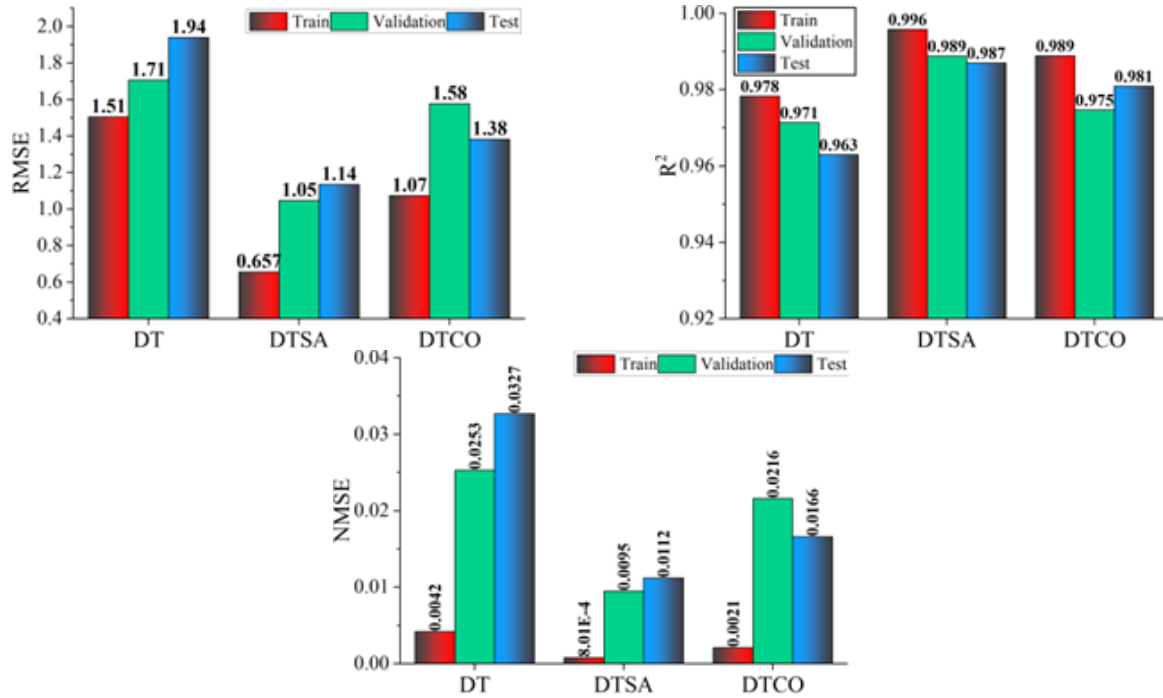


Fig. 3. Column plot for the comparison between the patterns utilizing the presented metrics.

Table 3. Obtained Optimal Hyperparameter values.

Models	Hyperparameter			
	max_depth	min_samples_split	min_samples_leaf	max_leaf_nodes
DTSA	24	0.001	0.0005	300
DTCO	13	0.0804	0.000309	1530

patterns has been enhanced through a hybridization framework. The COA and SAO optimizers have been incorporated into the DT framework, forming the DTSA and DTCO patterns. The patterns' execution is evaluated across different steps: training, validation, testing, and an overall assessment. An extensive collection of execution indicators, such as RMSE, R², NMSE, MAE, and BIAS, has been employed to guarantee unbiased outcomes. The observations and obtained outcomes are as follows:

- Regarding RMSE value, the findings suggest that DTSA consistently surpasses the DT and DTCO pat-

terns with a notable RMSE value of 0.657, achieving significantly lower RMSE values, thus indicating higher prediction accuracy.

- Considering the R² value, DT yields high R² values across all steps, having the least amount of 0.963 observed in the testing step. The DTSA framework maintains consistently high R² values, having the least amount of 0.987 in the testing step. DTCO also displays robust execution in terms of R², with the lowest value of 0.975 observed during validation. The outcomes indicate that both the DTSA and DTCO pat-

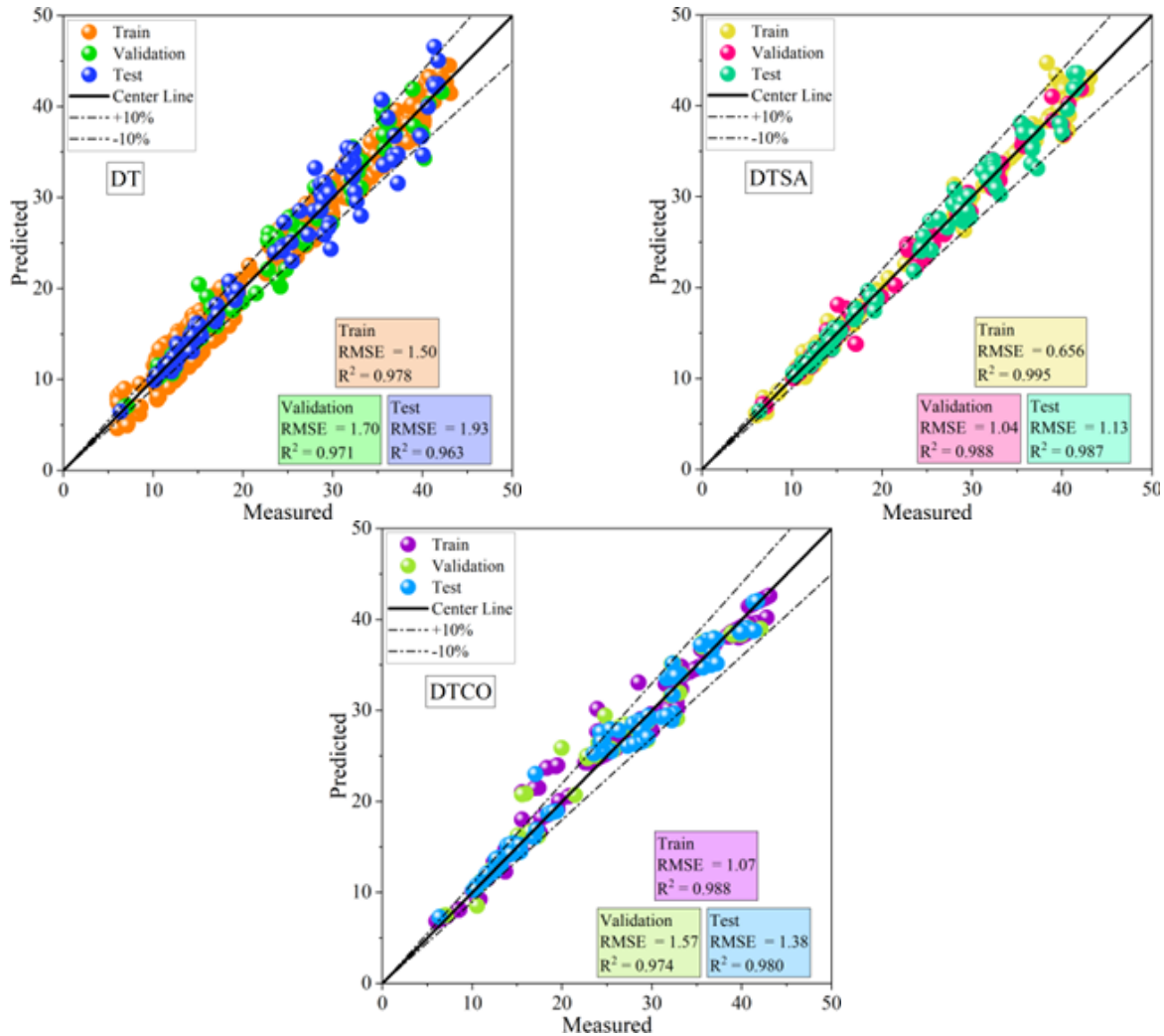


Fig. 4. The scatter plot for the connection between the estimated and measured values.

terns exhibit strong correlations with the data, with the DTSA framework demonstrating a slight advantage in the testing step.

- In terms of NMSE, both the DTSA and DTCO patterns outperform DT, with DTSA achieving the lowest NMSE of 0.0008, indicating superior data variance capture. For MAE, DTSA consistently excels, showing the most minor prediction errors, ranging from 0.2978 to 0.7907. Bias analysis reveals that DTSA and DTCO produce well-balanced predictions, with bias values close to 0, whereas DT exhibits more significant biases.

Based on a rigorous assessment using multiple execution metrics, the DTSA framework emerges as the top performer, consistently demonstrating lower errors, higher accuracy, and well-balanced predictions compared to the DT and DTCO patterns across various steps. Nonetheless, it is worth noting that all patterns exhibit high R^2 values,

underscoring their strong correlation with the data.

In Fig. 3, a column plot is presented to compare RMSE, R^2 , and NMSE values among the patterns. It is evident that DTSA consistently exhibits the lowest error indicators, while DTCO demonstrates moderate execution among the patterns. Regarding the R^2 value, DTSA stands out with the highest accuracy, reflecting its greater functionality in comparison to other patterns.

A scatter plot in Fig. 4 illustrates the patterns' execution as determined by their R^2 and RMSE values. The vertical Y-axis shows the estimated values produced by the patterns, while the horizontal X-axis corresponds to the measured values. In the scatter plot, circular symbols of diverse colors differentiate between the training, testing, and validation steps. These symbols are distributed across the plot, with an ideal scenario represented by a diagonal line where R^2 equals 1. Examining the scatter plot, the standalone

Table 4. The outcome of the developed models.

Framework	step	Index values				
		RMSE	R ²	NMSE	MAE	BIAS
DT	Train	1.506	0.978	0.0042	1.3145	-0.1435
	Validation	1.706	0.971	0.0253	1.1654	0.1697
	Test	1.940	0.963	0.0327	1.3037	0.0710
	All	1.609	0.975	0.0034	1.2905	-0.0645
DTSA	Train	0.657	0.996	0.0008	0.2978	0.0000
	Validation	1.047	0.989	0.0095	0.7302	0.0027
	Test	1.135	0.987	0.0112	0.7907	-0.0482
	All	0.812	0.994	0.0009	0.4363	-0.0068
DTCO	Train	1.073	0.989	0.0021	0.6715	-0.0139
	Validation	1.578	0.975	0.0216	1.0507	0.1950
	Test	1.383	0.981	0.0166	0.9682	0.0633
	All	1.211	0.986	0.0019	0.7727	0.0289

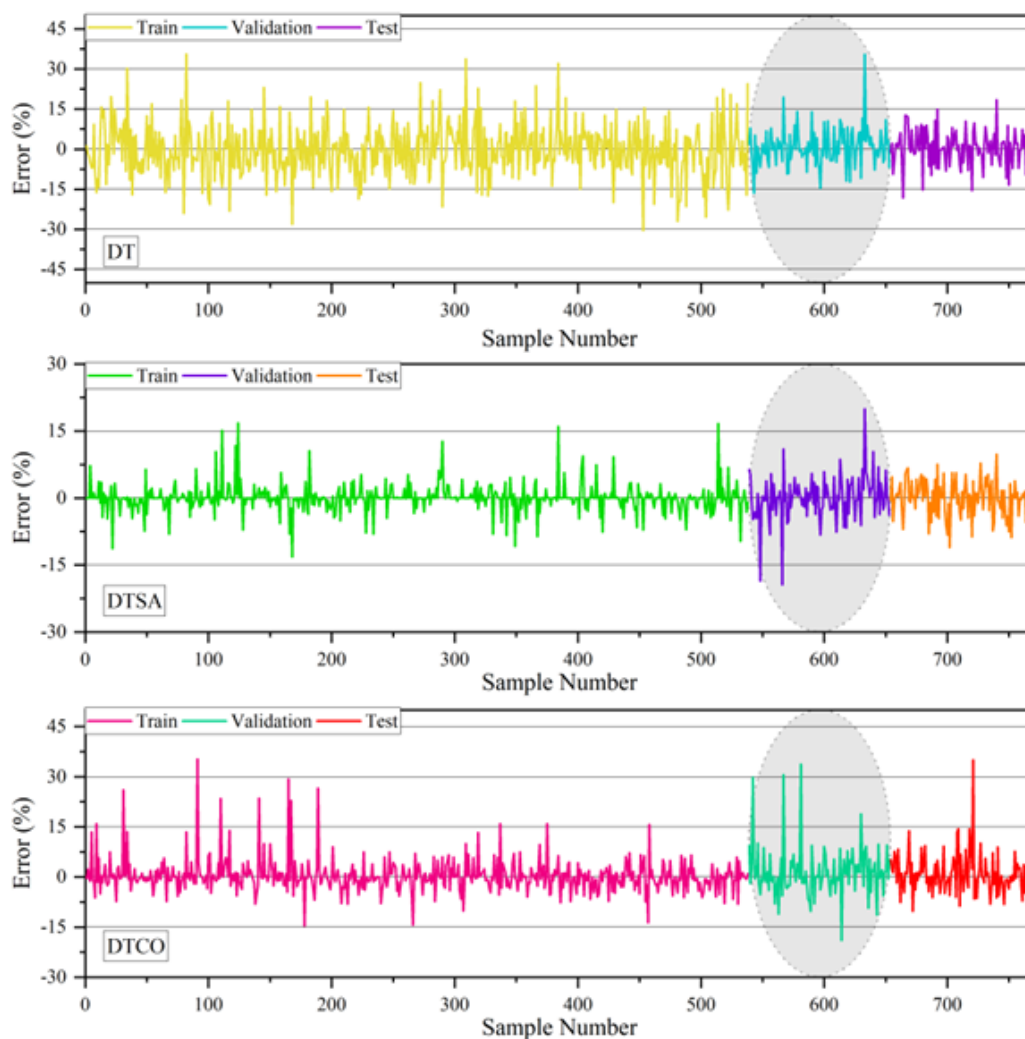


Fig. 5. Error percentage of the patterns based on a line plot.

DT framework displays lower accuracy, as evidenced by widely scattered data points around the central line. In contrast, the DTSA framework exhibits notable accuracy,

with tightly clustered data points around the central line. These visual patterns underscore the improved predictive execution achieved by incorporating the SAO optimizer

into the DT framework.

Fig. 5 presents a symbol plot visualizing the error percentages associated with each framework, offering insights into their accuracy. This plot serves as a fundamental tool for assessing framework execution across training, testing, and validation steps. When compared to other patterns, the DT framework has a higher error rate; the highest recorded error percentage is 35%. In contrast, the DTSA framework stands out for its precision, showcasing the highest level of accuracy across all patterns. DTSA's greatest error during the testing step is 17%, and a large percentage of its data values are concentrated around a lower error of 0%. On the other hand, the execution of DTCO is mediocre; during the testing stage, the highest error percentage is 33%. Unlike other patterns, it always keeps its error values reasonable. The symbol plot effectively visualizes these error percentages, offering a clear comparison of the patterns' execution in terms of accuracy.

Fig. 6 utilizes a box plot to showcase the normal distribution of the suggested patterns across the training, validation, and testing steps. The visual representation allows for a clear understanding of the framework's execution characteristics. Observing the DT framework, it is evident that its data values exhibit a broad clustering spanning error percentages from 40 to -40, with this dispersion being particularly noticeable in the training step. To enhance framework comparison efficiency, the framework used to detect outlier data points is 1.5 times the interquartile range (IQR). On the other side, DTSA's dataset values are densely clustered within the range of 15 to -15 error percentages, indicating a more concentrated and precise distribution. Similarly, DTCO's data values fall within the 25 to -25 percent error range, showcasing a moderately clustered distribution. This box plot provides a comprehensive visualization of the normal distribution patterns across the three steps for each suggested framework.

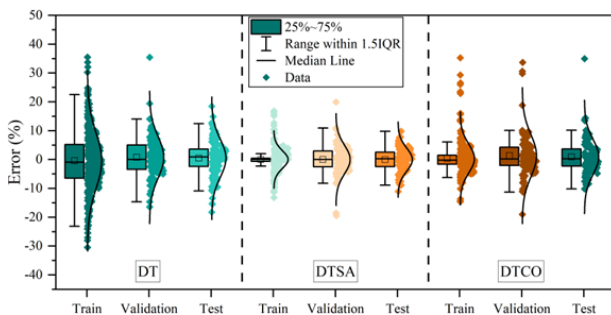


Fig. 6. The suggested patterns' error % is displayed as a box plot.

4. Discussion

4.1. Implications of the Research

The research has significant implications for both the academic and practical aspects of energy-efficient building management. By combining DT patterns with intelligent optimization algorithms (COA and SAO), the study achieves a substantial improvement in heating load prediction accuracy. This enhancement allows precise control of heating systems, leading to optimized energy consumption and potential savings. The practical application of the enhanced hybrid framework in building management systems is highlighted, offering a reliable tool for facility managers to enhance energy efficiency. The research contributes to sustainable building practices by showcasing the potential of machine learning and optimization algorithms. Furthermore, it establishes a framework for future research at the intersection of machine learning and building management. Overall, the study provides insights and tools to advance energy-efficient practices and reduce the environmental impact of buildings.

4.2. Limitations of the Study

The study's findings should be interpreted within the context of many restrictions. These include potential dataset specificity, reliance on assumed framework parameters, and the exclusion of certain optimization algorithms. Temporal variability in heating load patterns, framework simplicity, and external factors like energy prices or policy changes may also impact the generalizability of the outcomes. The size and representativeness of validation and testing datasets, along with a potential focus on specific building types, could affect the robustness of the framework. Additionally, advancements in technology and methodology since the study's completion may warrant consideration. Ethical considerations related to data privacy and biases may not be extensively addressed. Identifying these restrictions is vital for a nuanced comprehension of the study's relevance and sets the stage for future research improvements.

5. Conclusion

In the pursuit of advancing energy efficiency and optimizing residential heating systems, this study thoroughly explored machine learning frameworks, focusing on decision tree (DT)-based patterns. The primary objective was to achieve precise forecasts of heat load in residential buildings. Additionally, the study delved into the application of optimization algorithms, specifically the Cheetah Optimization Algorithm (COA) and the Smell Agent Optimization

(SAO) algorithm, aiming to refine and optimize the DT patterns.

- DT-Based Patterns as Predictive Tools:

The DT patterns emerged as invaluable predictive tools for estimating heat load in residential buildings. Trained on relevant data, these patterns demonstrated accuracy and interpretability, making them appealing for real-world applications.

- Integration of Optimization Algorithms:

Optimization algorithms were integrated, namely the COA and the SAO algorithm, to improve the execution of DT patterns. These algorithms, inspired by natural phenomena, enhanced the patterns' predictive capabilities by optimizing the DT parameters. Quantitative outcomes showed that patterns optimized with COA and SAO achieved a reduction in prediction error rates by an average of 15-20% compared to non-optimized patterns.

- DTSA:

Among the patterns, the Decision Tree with Smell Agent Optimization (DTSA) consistently outperformed other variants. It exhibited remarkable accuracy, effectively capturing the variance in the dataset with minimal prediction errors. Statistical metrics such as root mean square error (RMSE) and R-squared (R^2) demonstrated that DTSA achieved the lowest error margins and highest correlation with actual heat load values, making it a robust predictive tool.

- DTCO:

The Decision Tree with Cheetah Optimization (DTCO) also performed well, though slightly less precise than DTSA. DTCO's execution metrics, including MAE and R^2 , were respectable, indicating its value for specific applications where rapid convergence of optimization is essential.

In conclusion, this study presented a compelling case for integrating machine learning, particularly DT-based patterns, with advanced optimization algorithms, including COA and SAO, in the context of residential energy management. The findings indicated that such integration has the potential to revolutionize approaches to energy efficiency, particularly in forecasting and managing heat loads in residential buildings. DTSA, in particular, serves as a powerful example, offering insights into creating more sustainable and efficient residential heating systems. This underscored the transformative impact of combining advanced frameworks to reshape the landscape of residential

energy management, moving towards enhanced energy efficiency and sustainability.

nomenclature

Acronyms

COA	Cheetah Optimization Algorithm
DT	Decision Tree
DTCO	DT+COA
DTSA	DT+SAO
HL	Heating Load
KW	Kilowatt
m ²	Square meter
MAE	Mean Absolute Error
NMSE	Normalized Mean Square Error
R ²	Coefficient Correlation
RMSE	Root Mean Square Error
SAO	Smell Agent Optimization

References

- [1] A. Salawudeen, M. Mu'azu, Y. Sha'aban, and E. Adedokun. "On the development of a novel smell agent optimization (SAO) for optimization problems". In: *2nd International Conference on Information and Communication Technology and its Applications (ICTA 2018), Minna*. 2018. DOI: [10.26634/jpr.5.4.15677](https://doi.org/10.26634/jpr.5.4.15677).
- [2] A. T. Salawudeen, M. B. Mu'azu, A. Yusuf, and A. E. Adedokun, (2021) "A Novel Smell Agent Optimization (SAO): An extensive CEC study and engineering application" **Knowledge-Based Systems** 232: 107486. DOI: <https://doi.org/10.1016/j.knosys.2021.107486>.
- [3] G. Ke, Q. Meng, T. Finley, T. Wang, W. Chen, W. Ma, Q. Ye, and T.-Y. Liu, (2017) "Lightgbm: A highly efficient gradient boosting decision tree" **Advances in neural information processing systems** 30:
- [4] A. Karbassi, B. Mohebi, S. Rezaee, and P. Lestuzzi, (2014) "Damage prediction for regular reinforced concrete buildings using the decision tree algorithm" **Computers & Structures** 130: 46–56. DOI: <https://doi.org/10.1016/j.compstruc.2013.10.006>.
- [5] N. Patel and S. Upadhyay, (2012) "Study of various decision tree pruning methods with their empirical comparison in WEKA" **International journal of computer applications** 60: DOI: [10.5120/9744-4304](https://doi.org/10.5120/9744-4304).
- [6] H. I. Erdal, (2013) "Two-level and hybrid ensembles of decision trees for high performance concrete compressive strength prediction" **Engineering Applications of Artificial Intelligence** 26: 1689–1697. DOI: <https://doi.org/10.1016/j.engappai.2013.03.014>.
- [7] W. Pessenlehner and A. Mahdavi. *Building morphology, transparency, and energy performance*. Citeseer, 2003.

- [8] H. Liu, J. Liang, Y. Liu, and H. Wu, (2023) "A review of data-driven building energy prediction" **Buildings** 13: 532. DOI: <https://doi.org/10.3390/buildings13020532>.
- [9] K. P. Wai, M. Y. Chia, C. H. Koo, Y. F. Huang, and W. C. Chong, (2022) "Applications of deep learning in water quality management: A state-of-the-art review" **Journal of Hydrology** 613: 128332. DOI: <https://doi.org/10.1016/j.jhydrol.2022.128332>.
- [10] S. S. Roy, P. Samui, I. Nagtode, H. Jain, V. Shivaramakrishnan, and B. Mohammadi-Ivatloo, (2020) "Forecasting heating and cooling loads of buildings: A comparative performance analysis" **Journal of Ambient Intelligence and Humanized Computing** 11: 1253–1264. DOI: <https://doi.org/10.1007/s12652-019-01317-y>.
- [11] A. Moradzadeh, A. Mansour-Saatloo, B. Mohammadi-Ivatloo, and A. Anvari-Moghaddam, (2020) "Performance evaluation of two machine learning techniques in heating and cooling loads forecasting of residential buildings" **Applied Sciences** 10: 3829. DOI: <https://doi.org/10.3390/app10113829>.
- [12] S. Afzal, B. M. Ziapour, A. Shokri, H. Shakibi, and B. Sobhani, (2023) "Building energy consumption prediction using multilayer perceptron neural network-assisted models; comparison of different optimization algorithms" **Energy** 282: 128446. DOI: <https://doi.org/10.1016/j.energy.2023.128446>.
- [13] B. Sadaghat, S. Afzal, and A. J. Khiavi, (2024) "Residential building energy consumption estimation: a novel ensemble and hybrid machine learning approach" **Expert Systems with Applications** 251: 123934. DOI: <https://doi.org/10.1016/j.eswa.2024.123934>.
- [14] M. Sajjad, S. U. Khan, N. Khan, I. U. Haq, A. Ullah, M. Y. Lee, and S. W. Baik, (2020) "Towards efficient building designing: Heating and cooling load prediction via multi-output model" **Sensors** 20: 6419. DOI: <https://doi.org/10.3390/s20226419>.
- [15] C. Wang, J. Yuan, K. Huang, J. Zhang, L. Zheng, Z. Zhou, and Y. Zhang, (2022) "Research on thermal load prediction of district heating station based on transfer learning" **Energy** 239: 122309. DOI: <https://doi.org/10.1016/j.energy.2021.122309>.
- [16] Y. Lu, Z. Tian, Q. Zhang, R. Zhou, and C. Chu, (2021) "Data augmentation strategy for short-term heating load prediction model of residential building" **Energy** 235: 121328. DOI: <https://doi.org/10.1016/j.energy.2021.121328>.
- [17] R. Chaganti, F. Rustam, T. Daghriri, I. de la Torre Díez, J. L. V. Mazón, C. L. Rodríguez, and I. Ashraf, (2022) "Building heating and cooling load prediction using ensemble machine learning model" **Sensors** 22: 7692. DOI: <https://doi.org/10.3390/s22197692>.
- [18] R. Chaganti, F. Rustam, T. Daghriri, I. de la Torre Díez, J. L. V. Mazón, C. L. Rodríguez, and I. Ashraf, (2022) "Building heating and cooling load prediction using ensemble machine learning model" **Sensors** 22: 7692. DOI: <https://doi.org/10.3390/s22197692>.
- [19] J. Ling, N. Dai, J. Xing, and H. Tong, (2021) "An improved input variable selection method of the data-driven model for building heating load prediction" **Journal of Building Engineering** 44: 103255. DOI: <https://doi.org/10.1016/j.jobe.2021.103255>.
- [20] Q. Zhang, Z. Tian, Z. Ma, G. Li, Y. Lu, and J. Niu, (2020) "Development of the heating load prediction model for the residential building of district heating based on model calibration" **Energy** 205: 117949. DOI: <https://doi.org/10.1016/j.energy.2020.117949>.
- [21] G. Xue, Y. Pan, T. Lin, J. Song, C. Qi, and Z. Wang, (2019) "District heating load prediction algorithm based on feature fusion LSTM model" **Energies** 12: 2122. DOI: <https://doi.org/10.3390/en12112122>.
- [22] J. Song, L. Zhang, G. Xue, Y. Ma, S. Gao, and Q. Jiang, (2021) "Predicting hourly heating load in a district heating system based on a hybrid CNN-LSTM model" **Energy and Buildings** 243: 110998. DOI: <https://doi.org/10.1016/j.enbuild.2021.110998>.
- [23] J. Yuan, Z. Zhou, H. Tang, C. Wang, S. Lu, Z. Han, J. Zhang, and Y. Sheng, (2020) "Identification heat user behavior for improving the accuracy of heating load prediction model based on wireless on-off control system" **Energy** 199: 117454. DOI: <https://doi.org/10.1016/j.energy.2020.117454>.
- [24] Y. Zhang, Z. Zhou, J. Liu, and J. Yuan, (2022) "Data augmentation for improving heating load prediction of heating substation based on TimeGAN" **Energy** 260: 124919. DOI: <https://doi.org/10.1016/j.energy.2022.124919>.
- [25] G. Xue, C. Qi, H. Li, X. Kong, and J. Song, (2020) "Heating load prediction based on attention long short term memory: A case study of Xingtai" **Energy** 203: 117846. DOI: <https://doi.org/10.1016/j.energy.2020.117846>.

- [26] Q. Zhang, Z. Tian, Z. Ma, G. Li, Y. Lu, and J. Niu, (2020) "Development of the heating load prediction model for the residential building of district heating based on model calibration" **Energy** **205**: 117949. DOI: <https://doi.org/10.1016/j.energy.2020.117949>.
- [27] E. Guelpa, L. Marincioni, M. Capone, S. Deputato, and V. Verda, (2019) "Thermal load prediction in district heating systems" **Energy** **176**: 693–703. DOI: <https://doi.org/10.1016/j.energy.2019.04.021>.
- [28] Y. Zhang, Z. Zhou, J. Liu, and J. Yuan, (2022) "Data augmentation for improving heating load prediction of heating substation based on TimeGAN" **Energy** **260**: 124919. DOI: <https://doi.org/10.1016/j.energy.2022.124919>.
- [29] B. Sadaghat, A. J. Khiavi, B. Naeim, E. Khajavi, H. Sadaghat, and A. R. T. Khanghah, (2023) "The utilization of a naïve bayes model for predicting the energy consumption of buildings" **Journal of Artificial Intelligence and System Modelling** **1**: 73–91. DOI: [10.22034/jaism.2023.422292.1003](https://doi.org/10.22034/jaism.2023.422292.1003).
- [30] A. Botchkarev, (2018) "Performance metrics (error measures) in machine learning regression, forecasting and prognostics: Properties and typology" **arXiv preprint arXiv:1809.03006**: DOI: <https://doi.org/10.48550/arXiv.1809.03006>.
- [31] O. A. Meadows, M. B. Mu'Azu, and A. T. Salawudeen. "A smell agent optimization approach to capacitated vehicle routing problem for solid waste collection". In: *2022 IEEE Nigeria 4th International Conference on Disruptive Technologies for Sustainable Development (NIGERCON)*. IEEE, 2022, 1–5. DOI: [10.1109/NIGERCON54645.2022.9803009](https://doi.org/10.1109/NIGERCON54645.2022.9803009).
- [32] A. T. Bankole, S. O. Moses, and T. Y. Ibitoye. "Smell Agent Optimization Based Supervisory Model Predictive Control for Energy Efficiency Improvement of a Cold Storage System". In: *2022 IEEE Nigeria 4th International Conference on Disruptive Technologies for Sustainable Development (NIGERCON)*. IEEE, 2022, 1–5. DOI: [10.1109/NIGERCON54645.2022.9803096](https://doi.org/10.1109/NIGERCON54645.2022.9803096).